# Effect of Process Variables on Bead Geometry of the Submerged-Arc Strip-Overlay Welds

By R. S. Chandel and R. F. Orr*

## ABSTRACT

*A study has been made of the effect of process variables on the bead geometry and dilution in a submerged-arc strip-overlay process. Weld deposits were made on a 2.25 Cr-1 Mo steel plate using a 60 × .5 mm 309 L stainless steel strip. The effect of current, voltage, welding speed, electrode stickout, and preheat temperature was assessed on the bead width, bead height, penetration, and dilution. It was found that with the exception of preheat temperature all other variables had an influence on one or more features of the weld deposits. Welding parameters can be specified from these results so that a clad of any required shape and dilution can be deposited.*

*Metallographic examination revealed the microstructures in and adjacent to the fusion line and a microhardness survey was carried out to determine the hardness distribution in these areas.*

*A few deposits were analyzed by microprobe techniques and it was found that the welding conditions had a significant effect on the Ni and Cr content of the clad.*

## INTRODUCTION

Owing to their excellent mechanical properties and high resistance to corrosion and hydrogen attack, austenitic stainless steels are the obvious choice for reactor vessels in the petrochemical industry. However, because of the high cost of this meterial, fabrication of a complete vessel from austenitic stainless steel is not economic. Therefore, in normal practice a composite of low-alloy ferritic steel and an austenitic stainless steel is used. Such a composite provides an excellent balance of strength, surface properties, and economy. The barrier thickness of austenitic stainless steel required to resist corrosion and hydrogen attack on the base material is small compared to the total wall-thickness.

For fabrications that involve large clad areas such as pressure vessels, or where the base plate exceeds 100 mm in thickness, the only practicable method of cladding is weld deposition[1,2]. Various methods of cladding have been used for this purpose[3]. However, one of the most popular weld-deposition techniques is submerged-arc strip-cladding which has gained popularity in Europe and the U.K. This process deposits metal of excellent properties with limited dilution and the rate of deposition is high[3]. Furthermore, using a strip rather than a wire, reduces the number of overlapped regions, thus decreasing the number of sites for underclad cracking and other defects[4].

In principle, submerged-arc strip-cladding resembles submerged-arc welding except in strip-cladding a strip (normally 60 × 0.5 mm) is substituted for the round solid wire[5]. The other difference is that in strip-cladding the arc burns at a number of points along the strip edge, so that a high arc-force at a single point is not developed and this, in conjunction with the large weld-pool, means that the penetration of the base material is relatively low[6].

*The authors are with the Welding Sector of the Canada Centre for Mineral and Energy Technology, Ottawa, Canada. This was presented earlier at the Annual Conference of Canadian Institute of Metallurgists at Edmonton, Canada in August 1983.

To be satisfactory, a stainless-steel overlay should have the following characteristics [1,5,7].

(i) A guaranteed minimum thickness of cladding.

(ii) A minimum thickness of cladding within the specification for the stainless steel.

(iii) A suitable deposited microstructure and mechanical properties.

(iv) Complete fusion between parent metal and deposit.

(v) A finely rippled bead-surface, free from cracks, porosity, and slag inclusions.

The reasons for these requirements have been discussed elsewhere[3]. In submerged-arc strip-cladding they can be met by selecting a proper combination of strip, flux, and welding parameters. The process parameters that influence the cladding metallurgy and bead geometry are essentially the same as in conventional submerged-arc welding : namely current, voltage, welding speed, electrode stickout, preheat temperature, and electrode polarity. In strip-cladding the arc vibrates along the edge of the strip and it can be assumed that these welding parameters will influence the cladding chemistry and bead geometry differently. Many workers have attempted to established the relationship between process parameters and bead geometry, but there is a wide difference of opinion among them. Some have preferred high currents, voltages, and speeds, whereas others have preferred the opposite[5,8,9]. Very few have tried to isolate the influence of individual welding parameters on the geometry of the claddings. The aim of this work is a comprehensive study on the effect of each process variable on the shape and size of the strip-claddings. Evaluation of the optimum process-parameters to deposit a clad of the required specifications is an additional objective.

## EXPERIMENTAL TECHNIQUES

### Material

The experimental base material was a 2.25 Cr-1 Mo (SA-387 Grade 22 Class 2) steel which is generally used for the fabrication of pressure vessels because of its strength, toughness, and creep-resistance. The plate used was 12.6 mm thick and was supplied in the normalised and tempered condition. The chemical composition of the base plate is given in Table 1 and its microstructure is shown in Fig. 2. The plate was cut into $100 \times 300$ mm pieces and the surfaces were cleaned to remove dirt and oxides.
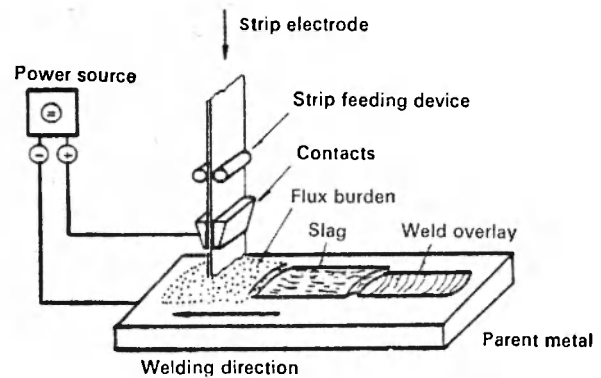
Fig. 1. Principle of Submerged-arc overlay process. (neg 4082)
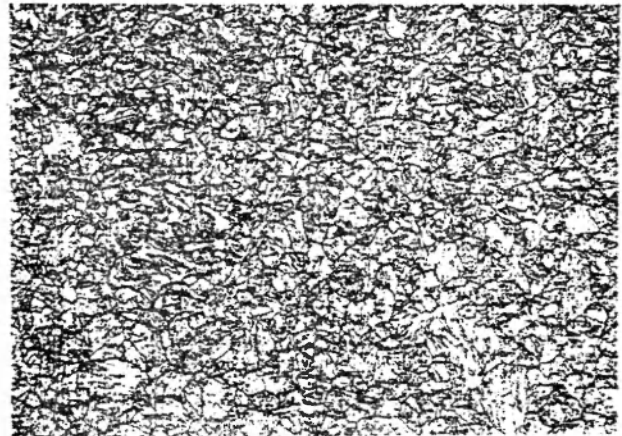
Fig. 2. Microstructure of parent metal-Etchant —2% nital $\times 300$. (neg 4168)

Weld deposits were made by using a $60 \times 0.5$ mm strip of 309 E stainless steel. This strip was in the form of 27-kg coils and its chemical composition is given in Table 1. A matching neutral and non-compensating type of flux was used for welding. Both the strip and flux were manufactured by Sandvik.

### Welding

A Lincoln SA-800 submerged-arc unit was used in conjunction with the Sandvik welding head suitable for strip widths of 60 to 120 mm. The power source was a D.C. generator with a variable potential which has the advantage of supplying an unfluctuating current.

During trial welding it was noticed that the 12.6 mm base plate, which had no backing, experienced excessive heating and distortion. To avoid this, a $600 \times 600$ mm jig was prepared from a 30 mm thick mild-steel plate and a copper shim, measuring $100 \times 300$ mm, was placed

## TABLE 1

### Chemical composition of materials (wt %)

| Material | C | Mn | Si | P | S | Ni | Cr | Cu | Mo | Al | Nb | Ti |
|----------|-----|------|------|-------|-------|-------|-------|------|------|-------|------|------|
| Strip (309 SS) | .052 | 1.56 | 0.64 | 0.026 | 0.008 | 10.43 | 19.37 | 0.06 | 0.24 | 0.017 | 0.02 | 0.01 |
| Base plate (SA 387 Grade 22 Class2) | 0.11 | 0.43 | 0.20 | 0.016 | 0.016 | — | 2.28 | — | 0.93 | — | — | — |

between the jig-plate and experimental plate to improve the heat transfer. Before welding the jig plate, the copper shim and experimental plates were tightened together to ensure adequate contact between them and to resist the distortion.

The flux was baked at 260°C for 2 h before use to remove moisture. Before the start of welding, the strip was cut at an angle of 20° to facilitate starting the arc and lowered to about 1.5 mm from the plate. Then flux was applied. Throughout the work the strip was held at 90° to the plate, and the electrode was positive. The normal length of the deposit was 285 mm.

To assess the influences of each process variable, a number of welds were made by varying each of the following five parameters while keeping the others constant : current, voltage, welding speed, electrode stickout, and preheat.

1. Varying the current and keeping voltage, speed, electrode stickout, and preheat constant.

2. Varying the voltage and keeping current, speed, electrode stickout, and preheat constant.

3. Varying the speed and keeping current, voltage, electrode stickout, and preheat constant.

4. Varying the electrode stickout and keeping current, voltage, speed, and preheat constant.

5. Varying the preheat and keeping current, voltage, speed and electrode stickout constant.

All of the welds were made twice and the results are given in Table 2.

## TABLE 2(a)

### Overlay bead characteristic as a function of current

| Weld No. | Current A | Bead width mm | Bead height mm | Penetration mm | Dilution (%) |
|----------|-----------|---------------|----------------|----------------|--------------|
| 1 | 600 | 60.04 | 2.57 | 1.00 | 28 |
| 2 | 600 | 59.66 | 2.77 | 0.78 | 22 |
| 3 | 650 | 61.94 | 2.93 | 1.20 | 29 |
| 4 | 650 | 61.75 | 3.29 | 0.79 | 20 |
| 5 | 850 | 63.84 | 4.28 | 1.41 | 25 |
| 6 | 850 | 62.70 | 4.00 | 1.06 | 21 |
| 7 | 1000 | 63.84 | 4.60 | 1.77 | 28 |
| 8 | 1000 | 62.90 | 5.55 | 1.48 | 21 |
| 9 | 1100 | 63.84 | 5.63 | 1.48 | 21 |
| 10 | 1100 | 62.32 | 5.77 | 1.40 | 20 |
| 11 | 750 | 62.70 | 3.39 | 0.91 | 21 |
| 12 | 750 | 63.84 | 3.87 | 1.08 | 22 |

## TABLE 2(b)

### Overlay bead characteristic as a function of voltage

| Weld No. | Voltage V | Bead width mm | Bead height mm | Penetration mm | Dilution (%) |
|---|---|---|---|---|---|
| 13 | 20 | 59.66 | 3.8 | 0.98 | 20.5 |
| 14 | 20 | 61.56 | 2.95 | 0.76 | 20.5 |
| 15 | 22 | 62.70 | 3.24 | 1.15 | 26.2 |
| 16 | 22 | 60.80 | 3.54 | 1.00 | 23.0 |
| 17 | 24 | 62.32 | 3.49 | 1.07 | 23.5 |
| 18 | 24 | 62.70 | 3.50 | 1.03 | 22.7 |
| 19 | 26 | 62.70 | 3.67 | 1.15 | 23.8 |
| 20 | 26 | 62.70 | 3.73 | 1.08 | 21.7 |
| 21 | 28 | 62.70 | 3.51 | 0.78 | 18.2 |
| 22 | 28 | 64.60 | 3.81 | 1.00 | 21.4 |
| 23 | 32 | 64.98 | 3.66 | 1.15 | 23.00 |
| 24 | 32 | 64.60 | 3.87 | 0.95 | 20.00 |
| 25 | 36 | 65.75 | 3.89 | 1.24 | 24.00 |
| 25 A | 36 | 67.00 | 3.73 | 1.37 | 27.00 |
| 26 | 40 | 64.60 | 3.88 | 1.28 | 24.8 |
| 26 A | 40 | 68.5 | 3.66 | 1.66 | 31.1 |

## TABLE 2(c)

### Overlay bead characteristic as a function of travel speed

| Weld No. | Travel speed mm/min | Bead width mm | Bead height mm | Penetration mm | Dilution (%) |
|---|---|---|---|---|---|
| 27 | 80 | 64.22 | 6.08 | 1.25 | 17.00 |
| 28 | 80 | 64.50 | 6.19 | 1.78 | 22.4 |
| 29 | 100 | 63.84 | 5.51 | 1.42 | 20.6 |
| 30 | 100 | 64.22 | 5.25 | 1.27 | 19.5 |
| 31 | 120 | 61.56 | 4.5 | 0.98 | 18.00 |
| 32 | 120 | 62.70 | 4.54 | 1.12 | 20.00 |
| 33 | 160 | 62.70 | 3.15 | 0.95 | 23.3 |
| 34 | 160 | 62.32 | 3.19 | 1.22 | 27.7 |
| 35 | 180 | 61.18 | 2.77 | 0.91 | 24.7 |
| 36 | 180 | 61.56 | 2.67 | 0.95 | 26.20 |
| 37 | 60 | 64.22 | 8.94 | 1.40 | 16.00 |
| 37 A | 60 | 63.80 | 8.54 | 1.45 | 14.50 |

## TABLE 2(d)

### Overlay bead characteristic as a function of preheat

| Weld No. | Preheat temperature °C | Bead width mm | Bead height mm | Penetration mm | Dilution (%) |
|---|---|---|---|---|---|
| 38 | 75 | 64.22 | 3.76 | 1.29 | 20.3 |
| 39 | 75 | 64.22 | 3.99 | 1.10 | 17.70 |
| 40 | 125 | 66.12 | 4.40 | 1.20 | 15.38 |
| 41 | 125 | 66.55 | 4.08 | 1.08 | 17.28 |
| 42 | 175 | 62.70 | 3.90 | 1.21 | 19.00 |
| 43 | 175 | 65.36 | 3.84 | 1.08 | 21.00 |
| 44 | 225 | 64.22 | 3.8 | 1.17 | 19.00 |
| 45 | 225 | 63.46 | 3.63 | 1.20 | 19.90 |
| 46 | 275 | 64.50 | 3.95 | 1.12 | 18.12 |
| 47 | 275 | 64.98 | 3.88 | 1.17 | 18.96 |

## TABLE 2(e)

### Overlay bead characteristic as a function of electrode stickout

| Weld No. | Electrode stickout | Bead width mm | Bead height mm | Penetration mm | Dilution (%) |
|---|---|---|---|---|---|
| 48 | 47.625 | 62.5 | 3.66 | 0.97 | 21.2 |
| 49 | 47.625 | 61.4 | 3.46 | 1.08 | 23.7 |
| 50 | 41.275 | 61.4 | 3.67 | 1.02 | 20.0 |
| 51 | 41.275 | 61.7 | 3.56 | 1.20 | 25.0 |
| 52 | 28.575 | 62.9 | 3.71 | 1.30 | 26.0 |
| 53 | 28.575 | 62.5 | 3.61 | 1.66 | 31.5 |
| 54 | 22.225 | 62.9 | 3.38 | 1.90 | 36.0 |
| 55 | 22.225 | 63.2 | 3.71 | 1.31 | 26.0 |

## Bead Measurements

Samples were cut from the centre of the weld across the width of the bead ; they were then polished and etched and the cross-section was photographed. The bead width, bead height, and penetration were measured from the enlarged photographs. These features are illustrated in Fig. 3. The dilution was calculated by using the following formula :

Dilution (%) $=\dfrac{P}{H+P} \times 100$, where P is penetration and H is bead height. These results are given in Table 2 and Fig. 3.
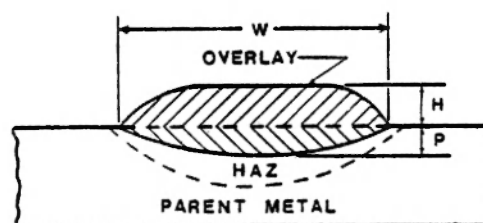


LEGEND
W—BEAD WIDTH
H—BEAD HEIGHT
P—PENETRATION

DILUTION $=\dfrac{P}{H+P}$

Fig. 3. Features of strip-overlay weld. (neg 3680)

## Metallography

Metallographic techniques were used to reveal the microstructures in the HAZ, fusion boundary, and clad layer. The structures in the base metal and HAZ were revealed by a 2% nital etch, and the ferrite and carbides in the overlay by electrolytic etching with a 2% chromic-acid solution. These micro-structures are shown in Fig. 2 and 6.

## Microhardness Survey

Microhardness measurements were carried out with a Tukon tester. Several hardness impressions were made on a straight line almost perpendicular to the fusion line. The impression-load was 500 g and the measurements were made in the parent metal, HAZ, fusion line, and clad layer. The results are shown in Fig. 5.

## Chemical Analysis

The distribution of alloying elements in and around the fusion boundary was determined by microprobe analyzer for welds made under optimum welding conditions. The elements of particular interest were Cr, Ni, Mn and Mo, and their distribution is shown in Fig. 7.

## RESULTS AND DISCUSSION

### Process variables and their influence on Bead Geometry

*Current*

Figure 4(a) shows bead width, bead height, penetration, and dilution as a function of current. When the current was increased from 600 to 1100 A, the bead width first increased until a current level of 750 A was achieved, and thereafter it remained constant. For the same variation of current, i.e., 600 to 1100 A, the bead height and penetration increased throughout the range ; the dilution, however, remained unchanged.

It is well established in submerged-arc welding that the current has the greatest influence on deposition rate and thus any change in welding current will have an
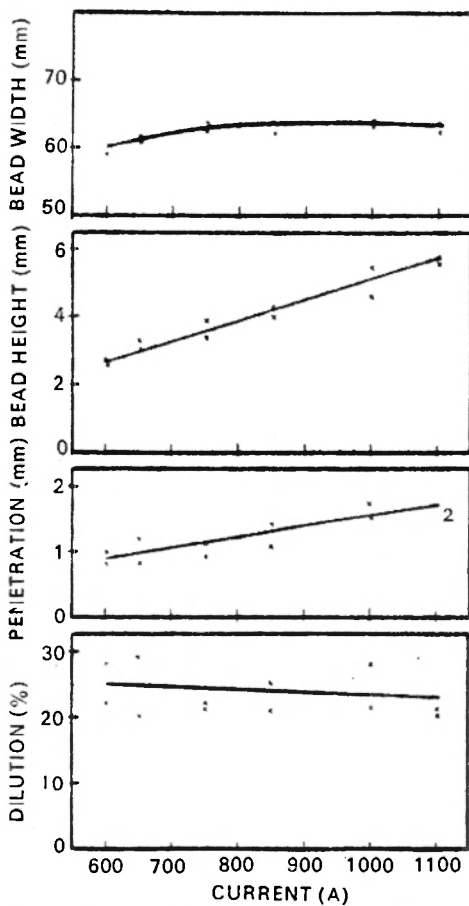


(a)  (neg 3750)

*Fig. 4(a). Relationship between welding speed and various features of weld overlay.*
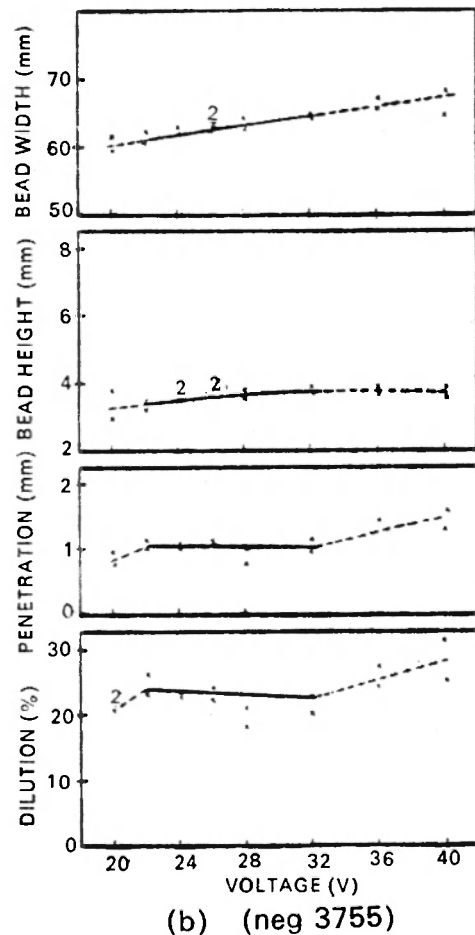


(b)  (neg 3755)

*Fig. 4(b). Relationship between welding voltage and various features of weld overlay.*
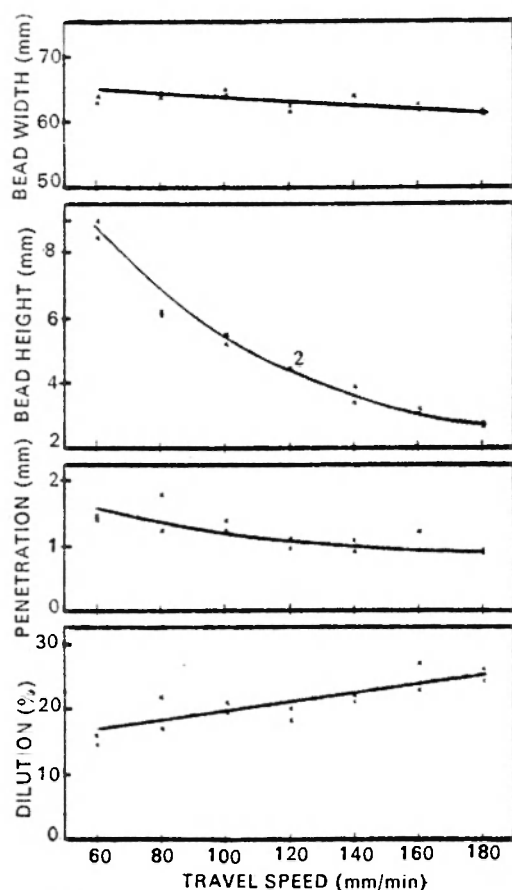
(c)  (neg 3753)

*Fig. 4(c).  Relationship between welding speed and various features of weld overlay.*



(d)  (neg 3752)

*Fig. 4(d).  Relationship between electrode stick-out and various features of weld overlay.*

influence on the bead height ; the results confirmed this[10]. The excess heat from the molten metal along with the heat of the arc, causes the base metal to fuse. The depth through which this fusion takes place is known as penetration. Higher current means greater energy for fusion and hence, greater penetration. Since the dilution is the ratio of the penetration to the total thickness of the fused metal (penetration plus bead height) and because the slopes of the curves of bead height and penetration are similar, therefore the dilution appear to be unaffected by the current.

*Voltage*

The curves in Fig. 4(b) show that when voltage was increased from 20 to 40 V, the bead width increased linearly but the bead height remained unaffected. The The penetration and dilution first increased when voltage was increased from 20 to 22 V, and then remained unchanged until the voltage reached 32 V. Between 32 and 40 V the penetration and dilution increased linearly.

In welding, the main function of the voltage is to control the arc length and the distribution of the energy. A higher voltage means a longer arc, and a larger area over which the molten metal is deposited, and consequently, wider beads—as observed. Because the voltage has little or no effect on the melting and deposition rate, the bead height was not affected.

Between 22 and 32 V the voltage has no effect on penetration and dilution which is in agreement with the results of Bush and Colvin[5] and Below[9]. However, between 20 and 22 V, and 32 and 40 V, the curves show that penetration and dilution increase with voltage. This is contrary to the principle of arc welding[10]. There are two probable reasons for this. First, during welding it was noticed that there were large fluctuations in current and voltage when the voltage was set too high or too low on the control panel. The second reason, as reported by Belov, is that when high values of voltage are used in submerged-arc welding, the conditions change to those of electroslag welding[9]. Further study of this

region is necessary to validate the specific reason(s) for this result.

## Speed

The welding speed is related to bead width, bead height, penetration, and dilution as shown in Fig. 4(c). Note that with increasing speed, bead width decreases slightly, while there is a marked decrease in bead height. Other effects are that penetration decreases and dilution increases.

Although the rate of melting remains unaffected, the arc travels a longer distance in unit time as the speed increases, and thus the same volume of molten metal has to be deposited over a larger area, and the weld bead will be thinner. The increase in speed also means less energy per unit area and consequently lower penetration. Since with increasing speed (or decreasing heat input) the bead height decreased much more rapidly than penetration, it is obvious that the dilution increased with increasing speed.
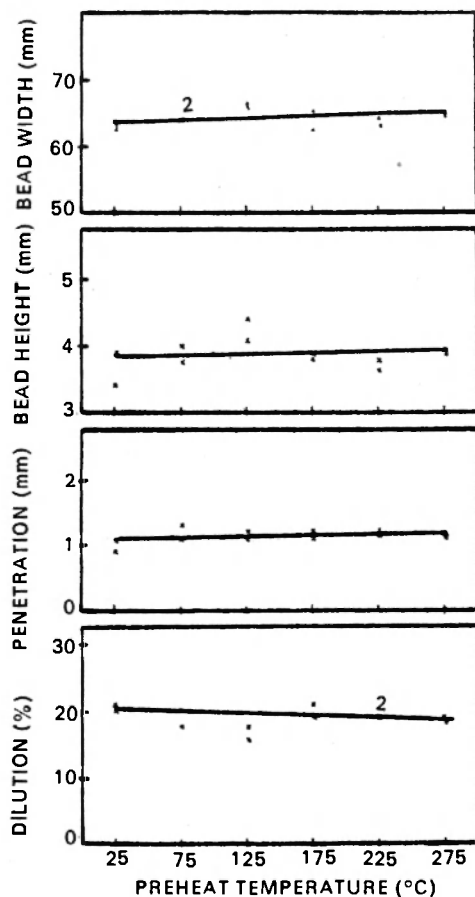


*Fig. 4(e).* Relationship between preheat temperature and various features of weld overlay. (neg 3756).

## Electrode stickout

Figure 4(d) shows that when electrode stickout was increased, the bead width and the bead height remained unaffected while the penetration and dilution decreased steadily. The results are to some extent in agreement with those of Reynolds who reported that in submerged-arc welding the electrode stickout influenced both the bead height and the penetration[11]. This discrepancy probably arises because when the electrode stickout is increased for the same equipment settings, the current automatically decreases from the increased resistance of the electrode. In future work the current should be adjusted during welding to take account of this factor.

## Preheating temperature

The curves in Fig. 4(e) represent the relationship between preheat temperature and bead width, bead height, penetration, and dilution. They show that preheat temperatures of up to 275°C have no significant effect on any of the bead features. This is probably because the heat input from preheating was small compared to the heat input of the process.

## MICROSTRUCTURE AND HARDNESS DISTRIBUTION

Figure 2 shows the microstructure of the parent metal, and those of the HAZ, fusion line and overlay are shown in Fig. 6. The parent metal has a tempered bainitic structure with some ferrite. The microstructure within the HAZ consists of ferrite and bainite, with an increasing proportion of bainite closer to the fusion line. The increase in bainite is consistent with the peak temperature increasing as the fusion line is approached. Near the fusion line where the temperature exceeds $Ac^3$, there are some signs of grain growth, [(Fig. 6(b)].
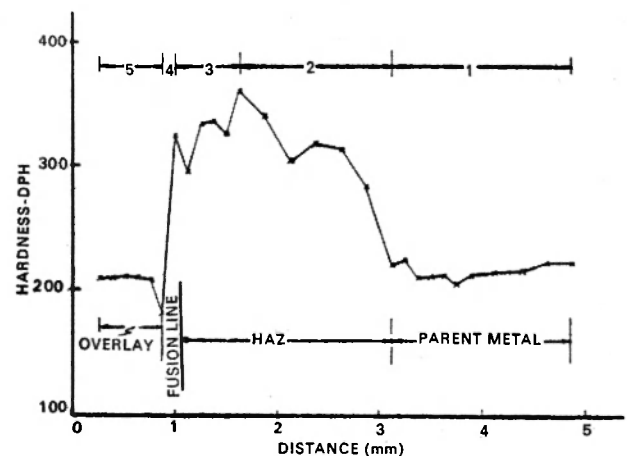


*Fig. 5.* Distribution of microhardness in a weld overlay. (neg 3756)

In the overlay, the microstructure is austenitic with 5-10% ferrite and some carbides, [Fig. 6(a)].

Figure 5 shows the microhardness values in and adjacent to the fusion line of the weld overlay. The curve can be divided into five distinct zones. Moving from right to left, the first flat part is representative of the base metal and shows almost uniform hardness. Adjacent to it is the HAZ, where the hardness steadily increases to a peak value of 360 D.P.H. The peak hardness is related to the high percentage of bainite. In zone three, the hardness decreases to 300 D.P.H. as the grain size increases.

The dramatic drop in the hardness in zone four is probably from a sudden change in the chemical composition near the fusion line, from that of 2.25 Cr-1 Mo to a 309 L stainless steel. In zone five the hardness curve is flat and is representative of the hardness of the deposited 309 L stainless steel.

## CHEMICAL COMPOSITION OF THE FUSION AND OVERLAY REGIONS

The distribution of Cr, Ni, Mn and Mo as determined by the microprobe analyzer for the fusion and overlay regions of "as-welded" joints is shown in Fig. 7. It can



(a) clad etchant 2%
chromic acid
(neg 4167)

*Fig. 6(a). Microstructures in a weld overlay.* ×500



(b) fusion line Etchant
2% nital (neg 4166)

(c) HAZ Etchant 2% nital
(neg 4169)

*Fig. 6(b) & 6(c). Microstructures in a weld overlay.* ×500
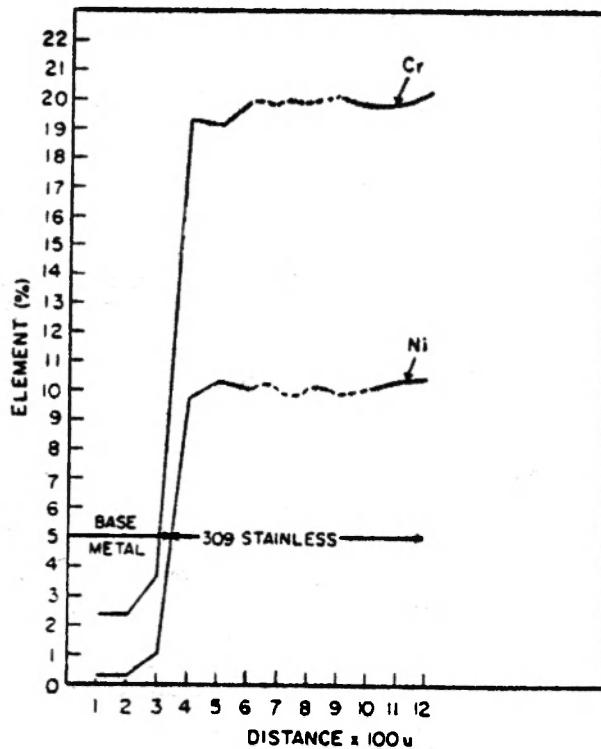
Fig. 7(a). Distribution of Cr & Ni in a weld
overlay joint (neg 8677)
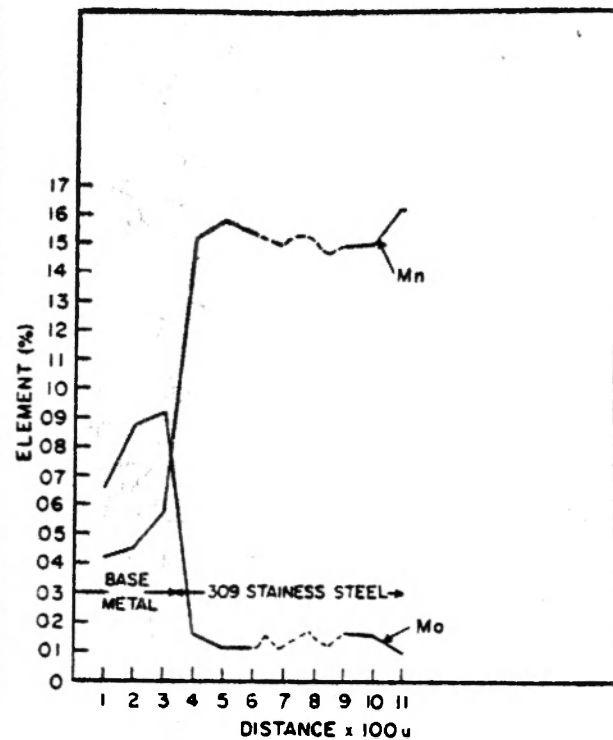


Fig. 7(b). Distribution of Mn and Mo in a
weld overlay joint (neg 8677)

be seen that on the overlay side, the Cr, Ni, and Mn contents quickly rise over a distance of 100 $\mu$m. At the same time, the Mo content falls. The narrow fusion zone and the uniformity of Cr, Ni, Mn and Mo contents thereafter indicate the fused metal attains chemical equilibrium within a relatively short distance. The chemical composition of the overlay also suggests that the Co, Ni and Mn requirements can be achieved in a single layer overlay by using 309 L stainless steel. However, the use of single layer overlay is restricted because of carbon pick up from the base metal. It would be useful to know the carbon distribution of the first layer, however it is not easily measured by microprobe analyzer.

## CONCLUSIONS

1. An increase in current resulted in an increase in bead height and penetration, but the bead width and dilution remained unchanged.

2. Increasing the welding voltage caused the bead width to increase but other features were unaffected.

3. When welding speed was increased, the bead height and penetration decreased but dilution increased.

4. Electrode stickout does not seem to have any effect on bead width and bead height, but when it was increased, both the penetration and dilution increased.

5. Preheat temperatures up to 275°C did not affect any of the weld features.

6. From this study it can be concluded that the following welding parameters will produce a clad of low dilution, complete bonding and with adequate microstructure both in HAZ and clad.
   Current—850 A
   Voltage—26 V
   Speed—140 mm/min
   Electrode stickout—35 mm
   No preheat

7. The microhardness increased steadily in the HAZ to a peak then decreased slightly. At the fusion line there was a dramatic drop in hardness.

8. Metallographic examination revealed the bainitic structure of the HAZ near the fusion boundary, and the austenitic structure with some ferrite and carbodes in the clad.

## ACKNOWLEDGEMENTS

## REFERENCES

1. Marshal, A. B., Jordan, M. F. and Aston, J. L. *Welding and Metal Fabircation*, 41:8:292 ; 1973.

2. Zentner, H. *Ibid*, 44:4:208 ; 1976.

3. Gooch, T. G. *Welding Research Abroad*, 24:6:3 ; 1978.

4. Lavigne, M. J. "Possible Designs and Manufacturing Sequences for a 10,000 Barrel/Day Hydrogenation Vessel for Up-Grading Heavy Oils and Tar Sands Bitumen", *Lab Report* MRP/PMRL 79-70 (TR), CANMET, Energy, Mines and Resources Canada ; 1979.

5. Bush, A. F. and Colvin, P. *Welding and Metal Fabrication*, 37:6:234 ; 1969.

6. Almgvist, G. and Egeman, N. *Ibid*, 31:7:294 ; 1963.

7. Horsefield, A. M., Almgvist, G. and Rosendahl, C. H. *Br. Weld. J.*, 13:5:315 ; 1966.

8. Forsberg, S. and Pollak, P. "Technical and Practical Aspects of Submerged-Arc Surfacing with Strip Electrodes", Sandvik, Sweden, 1979.

9. Belov, Yu. M., *Svar Priozvod*, 12:7: ; 1961.

10. Welding Handbook, Section 2, 28:40 ; American Welding Society, 1963.

11. Reynolds, D. E. H. Submerged Arc Welding, Edited by S. B. Jones, 43-48, The Welding Institute, 1978.